



Evaluating the Environmental Impacts of Urban Sprawl in Xiamen, China

HUANG Suqi + Lin Zhewei + SHI Kaiwen + Zhu Houhua

Spring 2022

Content

| | |
|---|-----------|
| 1. Background | 3 |
| 2. Literature Review | 3 |
| 2.1 Urban expansion | 3 |
| 2.2 Ecological Evaluation Index | 4 |
| 2.3 Utilize RSEI to evaluate Urban Expansion | 4 |
| 2.4 Artificial Intelligence in evaluating ecological environment | 4 |
| 3. Study Context | 5 |
| 4. Study Area and Data explanation | 6 |
| 4.1. Study area | 6 |
| 4.2. Land-use data | 6 |
| 4.3. Remote Sensing Data | 6 |
| 4.3.1. Landsat-8 OLI data | 6 |
| 4.3.2. Data preprocessing | 7 |
| 5. Urban expansion Characteristics of Xiamen from 2010 to 2020 | 8 |
| 5.1. Urban expansion metrics | 8 |
| 5.1.1. Proportion of Construction Land | 8 |
| 5.1.2. Urban expansion Intensity Index | 8 |
| 5.1.3. The Land Use Transfer Matrix | 8 |
| 5.2. Analysis of urban expansion process | 8 |
| 5.2.1. Analysis of built-up area | 8 |
| 5.2.2. Conversion from the artificial surface to other land-use types | 9 |
| 5.2.3. Conversion from other land-use types to the artificial surface | 9 |
| 6. Eco-environmental quality assessment | 10 |
| 6.1. RSEI Model | 10 |
| 6.1.1. Principle of the RSEI Model | 10 |
| 6.1.2 Indicator selection | 10 |
| 6.1.3 PCA Analysis | 12 |
| 6.1.4. RSEI Model Building | 12 |
| 6.2. PCA Result | 12 |
| 6.3. Evaluation of Ecological Environment | 13 |
| 6.4. Case study of ecological change | 16 |
| 7. Conclusion | 19 |
| Reference | 20 |

1. Background

In recent years, rapid urbanization in China has been studied by many researchers. To satisfy the economic development demand and growing urban population, the urbanization speed in China has reached a high condition. Especially in east coast cities, the high urbanization rate has brought huge changes, including city image, urban form, landscape, etc. Although the urbanization process has promoted economic development and civilization level, many essential fields such as ecological environment and natural resource protection have been overlooked.

Xiamen is a prefecture-level city in Fujian Province and was one of China's earliest coastal economic special zones. After around 40 years of rapid development, Xiamen has reached many economic accomplishments and a nearly 90% of urbanization rate. The urbanization area has been expanded from old town Xiamen to surrounding areas. And urban expansion occurred during the urbanization process.

Located in the south of China, Xiamen city is covered by a tropical monsoon climate, with great ecological environments and resources. However, the urbanization process transferred land use turned natural land into hardened land, and vegetation cover turned into built-up areas. With insufficient urban planning during rapid economic development, the ecological damage cannot be neglected to achieve long-term sustainable development for the city.

Therefore, this study would be started from both urban expansion phenomena and ecological environment evaluation by utilizing remote sensing images, identifying urban expansion conditions and ecological environment change to analyze the impact of urban expansion from an environmental aspect.

2. Literature Review

2.1 Urban expansion

Urban expansion is commonly discovered during the urbanization process, which is regarded as one of the urban growth appearances. During the fast urbanization, the demand for residential areas is rising higher than urban planning, which causes urban expansion with unplanned or insufficient planning context. Several reasons are caused by a growing population, rising incomes, falling commuting costs, etc. (Brueckner, 2000). Meanwhile, urban expansion may cause several side effects, such as sub-urbanization, land fragmentation, and ecological degeneration (Irwin and Bockstael, 2007). When evaluating the urban expansion phenomenon, the side effect would be addressed more in order to understand urban development.

2.2 Ecological Evaluation Index

The ecological environment is complicated to evaluate in a comprehensive view. The ecological environment evaluation is diverse based on different criteria, including forest, water bodies, land cover, etc. Many indexes have particular evaluation purposes in each field, and there are several classical indexes (Pettorelli *et al.*, 2005) :

- (1) EVI: Enhanced Vegetation Index
- (2) GVI: Global Vegetation Index
- (3) LAI: Leaf Area Index
- (4) NDVI: Normalized Difference Vegetation Index
- (5) SAVI: Soil Adjusted Vegetation Index
- (6) EI: Ecological index

2.3 Utilize RSEI to evaluate Urban Expansion

When building the connection between ecological index evaluation and the urban expansion phenomenon, several scholars have applied the RSEI model to classify different landscape elements (Hu and Xu, 2018). The RSEI is an index based on greenness, humidity, heat, and dryness indicators and is therefore based on remote sensing information and natural factors so that it can quickly and easily evaluate regional ecological quality. Ecological quality. During the urban expansion process, mass rural land or natural environment has been changed into the urban construction area. To identify urban expansion, land-use and land cover change could be observed by remote sensing data, utilizing remote sensing images (Tang, Wang and Yao, 2006). The RSEI can not only be used as a quantitative indicator to portray regional ecological quality but can also visualize regional ecological quality, allowing spatial and temporal analysis, simulation, and prediction of regional ecological changes, and can be used regardless of time and space constraints, and can therefore make up for the shortcomings of the EI index in these areas.

2.4 Artificial Intelligence in evaluating ecological environment

Artificial intelligence, especially computer vision techniques, has been frequently applied in recent years to help identify huge image datasets into an analytical dataset. Remote sensing data are utilized to analyze land use and land cover change. By analyzing the land cover change in years, the urban expansion direction and side effects on the ecological environment could be discovered (Xu *et al.*, 2018). However, the remote sensing dataset usually has large raw data, so the cleaning process conducted by humans would cost too much. The trained artificial intelligence would assist human beings in processing the remote sensing data, saving data process and cleaning time and cost.

3. Study Context

The research flow path would be conducted in two paths, the urban expansion character identification and ecological quality evaluation process, and the final result of the urban expansion impact on ecology environment would be analyzed with the actual site to study the specific impact on the micro-level. (Figure 3.1.1).

Urban expansion characteristic identification: Based on the land utilization data collected in 2010 and 2020, to analyze the proportion of construction land and urban expansion intensity and land utilization change in Xiamen. The urban expansion identification would utilize two periods of land use data, six types of land use, to analyze construction land proportion, urban expansion degree, construction land, and other uses of land condition.

Ecological quality evaluation: The ecological quality evaluation dataset could utilize 9 time periods of remote sensing data source, selecting Landsat8 image data from 2013 to 2021, utilizing the RSEI model to quantitative evaluate the ecological quality in Xiamen, and analyze the impact of urban expansion on ecology quality. Applying the RSEI model and PCA analysis could identify the primary components to analyze the urban expansion.

The RSEI model is used to simulate and predict this research's regional ecological change trends. Firstly, the thematic images of NDVI, Wet, LST, NDSI, and RSEI were sampled for each year, and then stepwise regression analysis was carried out with RSEI as the dependent variable and NDVI, Wet, LST, and NDSI as the independent variables to establish their relationship models. A 5x5 grid was used with 28,000 sample points collected for each image. A large number of sample points and the sampling method across the whole image can ensure the representativeness and objectivity of the regression analysis results and avoid the uncertainty of the results caused by small samples and local sampling.

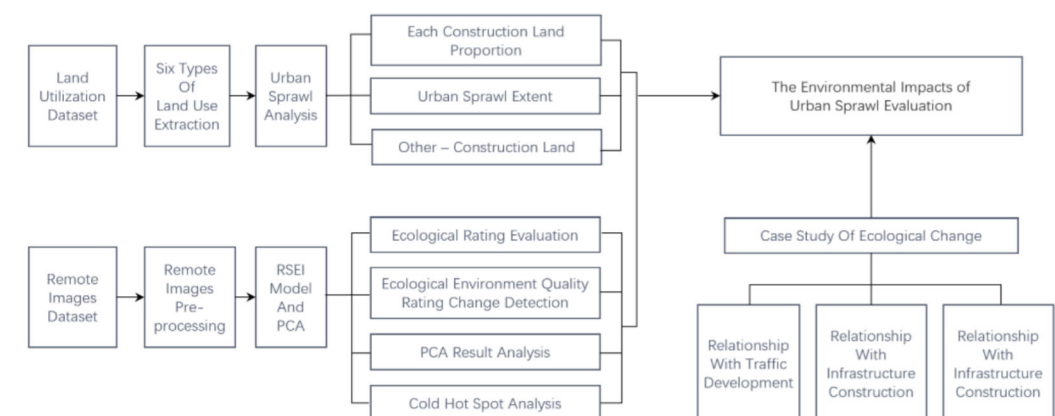


Figure 3.1.1 Research workflow

4. Study Area and Data explanation

4.1. Study area

This study selects Xiamen city as the study area, located in the south of Fujian Province, China. The topography of Xiamen is mainly plains, hills, and terraces, with high terrain in the northwest and low landscape in the southeast, while hills, terraces, marine plains, and mudflats in the northwest to southeast, in that order.

4.2. Land-use data

The GlobeLand30 land use data for 2010 and 2020 in Xiamen were selected for this study. GlobeLand30 is a publicly available global land cover data developed by China with a spatial resolution of 30 m, using the WGS-84 coordinate system. This study contains six land-use types: Cropland, Forest, Grass, Shrub, Water bodies, and Artificial surface. The GlobeLand30 land use classification map of Xiamen in 2010 and 2020 is shown in Figure 4.2.1.

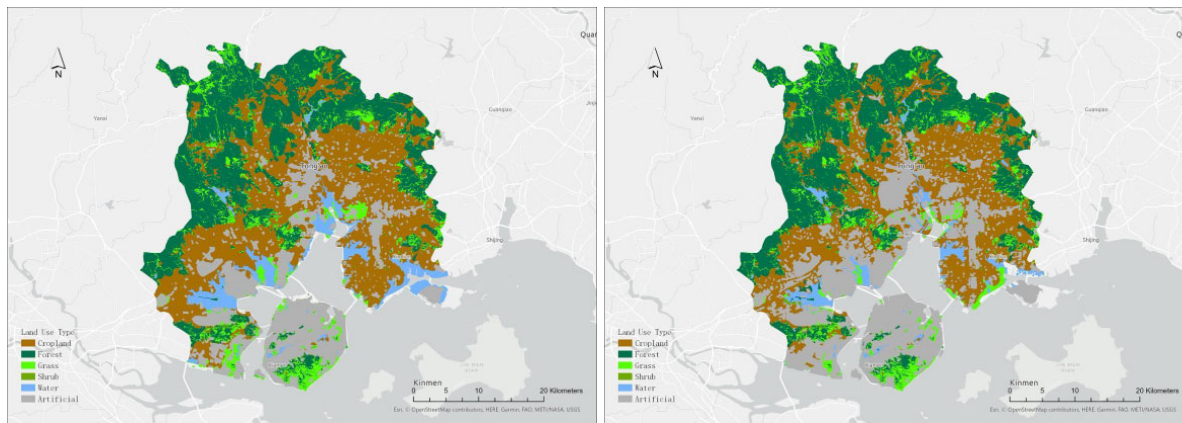


Figure 4.2.1 (a)

Figure 4.2.1 (b)

Figure 4.2.1 (a) GlobeLand30 in 2010; (b) GlobeLand30 in 2020

4.3. Remote Sensing Data

4.3.1. Landsat-8 OLI data

The remote sensing image data selected for this study are Landsat-8 OLI data, and the image data are obtained from the USGS website. (<https://landsatlook.usgs.gov/>).

This study uses nine remote sensing images covering Xiamen (path 119, row 43) in different years. And Xiamen belongs to the subtropical maritime monsoon climate, so it is rainy and cloudy in summer, with solid cloud disturbance and poor meteorological conditions. For this situation, the remote sensing images selected are all between January and March to reduce the impact of climate, with cloudiness below 5% for the study. Table 4.3.1 shows the remote sensing image information table for nine periods.

Table 4.3.1 Information of nine remote sensing image

| Satellite Name | Data Number | Date Obtained | Cloud Volume |
|----------------|--|---------------|--------------|
| Landsat 8 | LC08_L1TP_119043_20130323_20170429_01_T1 | 2013-03-23 | 3.65% |
| | LC08_L1TP_119043_20140127_20170426_01_T1 | 2014-01-27 | 4.94% |
| | LC08_L1TP_119043_20150114_20170414_01_T1 | 2015-01-14 | 2.89% |
| | LC08_L1TP_119043_20160305_20170328_01_T1 | 2016-03-05 | 4.71% |
| | LC08_L1TP_119043_20170103_20170312_01_T1 | 2017-01-03 | 2.11% |
| | LC08_L1TP_119043_20180311_20180320_01_T1 | 2018-03-11 | 2.98% |
| | LC08_L1TP_119043_20190125_20190205_01_T1 | 2019-01-25 | 4.01% |
| | LC08_L1TP_119043_20200316_20200326_01_T1 | 2020-03-16 | 4.89% |
| | LC08_L1TP_119043_20210215_20210304_01_T1 | 2021-03-04 | 0.29% |

4.3.2. Data preprocessing

There are two steps for pre-processing Landsat-8 OLI data: radiometric calibration and atmospheric correction.

- (1) Radiometric calibration converts the DN values of the original images to the outer atmospheric surface reflectance, which eliminates the interference from the solar altitude angle, the sensor itself, and the atmosphere.
- (2) Atmospheric correction converts the surface reflectance or radiance brightness values into the actual surface reflectance. It can effectively eliminate the errors caused by various environmental factors such as absorption or scattering of the atmosphere and illumination and obtain more accurate parameters such as surface temperature, radiance, and reflectance.

The remote sensing image before and after pre-processing is shown in Figure 4.3.2.



Figure 4.3.2 (a)

Figure 4.3.2 (b)

Figure 4.3.2 (a) Remote sensing image before pre-processing; (b) Remote sensing image after pre-processing (taking the remote sensing image of the 2018 year as an example)

5. Urban expansion Characteristics of Xiamen from 2010 to 2020

5.1. Urban expansion metrics

In this study, three urban expansion metrics are applied.

5.1.1. Proportion of Construction Land

The proportion of Construction Land (PCL) is the percentage of the total construction area in a given city in a given year, used to quantify the actual situation of urban expansion. The formula is as follows.

$$PCL = \frac{B_{construction}}{B_{total}}$$

Where $B_{construction}$ is the area of the construction land for that year, B_{total} is the total planning land area of the city for that year. The higher value of PCL represents a higher level of urbanization.

5.1.2. Urban expansion Intensity Index

The urban expansion Intensity Index (UII) is the percentage of a spatial unit's expansion over its total urban land area during the study period. It compares the intensity and speed of urban expansion over time. The formula is as follows.

$$UII = \frac{\Delta B}{B_{total} \times T} \times 100\%$$

Where ΔB is the increase in the area of construction land in any two years before and after, B_{total} is the total area of the study area. The urban expansion intensity results were classified according to the resulting values into five classes: high speed ($UII > 1.92$), fast ($1.05 < UII \leq 1.92$), medium speed ($0.59 < UII \leq 1.05$), low speed ($0.28 < UII \leq 0.59$), and slow ($0 < UII \leq 0.28$).

5.1.3. The Land Use Transfer Matrix

The land Use Transfer Matrix is the interconversion of land use types in the same region over different periods, generally presented in a two-dimensional table, and the specific situation of interconversion between each land type can be quickly observed.

5.2. Analysis of urban expansion process

5.2.1. Analysis of built-up area

According to PCL, Xiamen's overall construction land ratio increased from 19.44% in 2010 to 27.8% in 2020. Specifically, Xiamen's construction land increased from 307.09 km² in 2010 to 439.61 km² in 2020, increasing 132.52 km². And the UII of Xiamen is 0.08 during the period from 2010 to 2020. The expansion of the built-up area from 2010 to 2020 is shown in Figure 5.2.1.

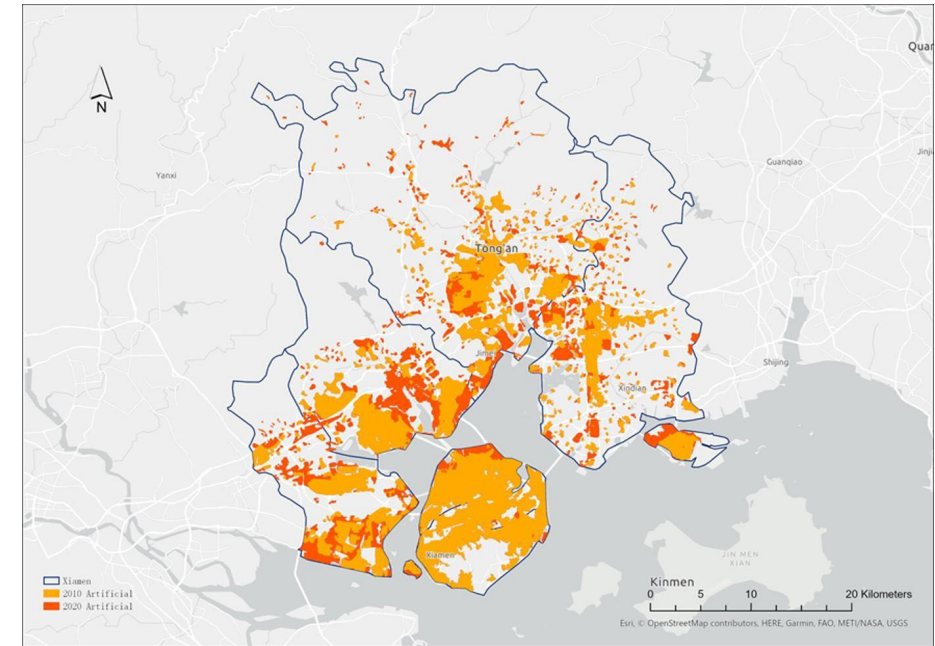


Figure 5.2.1 Expansion map of construction area

5.2.2. Conversion from the artificial surface to other land-use types

As Table 5.2.2 shows that 13.95 km² of the artificial surface was converted to cropland, forestland, grassland, and shrubland over ten years, with the most significant percentage of 8.45 km² being the type converted from artificial surface to cropland. And in 2020, 8.9km² of wetlands were added compared to 2010, which is a significant improvement to the ecological environment.

Table 5.2.2 Land use type conversion table (Unit: km²)

| 2010/2020 | Grass | Cropland | Shrub | Forest | Artificial | Wetland | Water | Sum |
|-------------------|---------|----------|-------|---------|------------|---------|--------|----------|
| Grass | 78.543 | 4.774 | 1.008 | 28.880 | 16.373 | 0.686 | 1.021 | 131.285 |
| Cropland | 5.490 | 417.100 | 0.107 | 9.133 | 93.566 | 0.353 | 3.243 | 528.993 |
| Shrub | 1.034 | 0.129 | 1.565 | 0.985 | 0.954 | 0.103 | 0.399 | 5.169 |
| Forest | 29.401 | 8.821 | 0.992 | 447.822 | 4.135 | 0.007 | 0.794 | 491.973 |
| Artificial | 3.081 | 8.451 | 0.227 | 0.806 | 292.923 | 0.613 | 0.773 | 306.875 |
| Water | 7.460 | 4.872 | 1.450 | 0.936 | 23.303 | 8.405 | 46.241 | 92.667 |
| 总计 | 125.009 | 444.148 | 5.350 | 488.562 | 431.255 | 10.166 | 52.471 | 1556.961 |

5.2.3. Conversion from other land-use types to the artificial surface

As Figure 5.2.3 displays, from 2010 to 2020, the total area of urban expansion was 132.526 km², of which 12.7% was occupied grassland, 70.9% cropland, 3.1% forest land, 0.7% shrubland, and 17.7% water bodies. In summary, 2010-2020 urban expansion was mainly carried out by occupying cropland and water bodies. As a result, people reclaimed ecological lands to increase the amount of cropland to ensure agricultural production, leading to a vicious circle of ecological environment

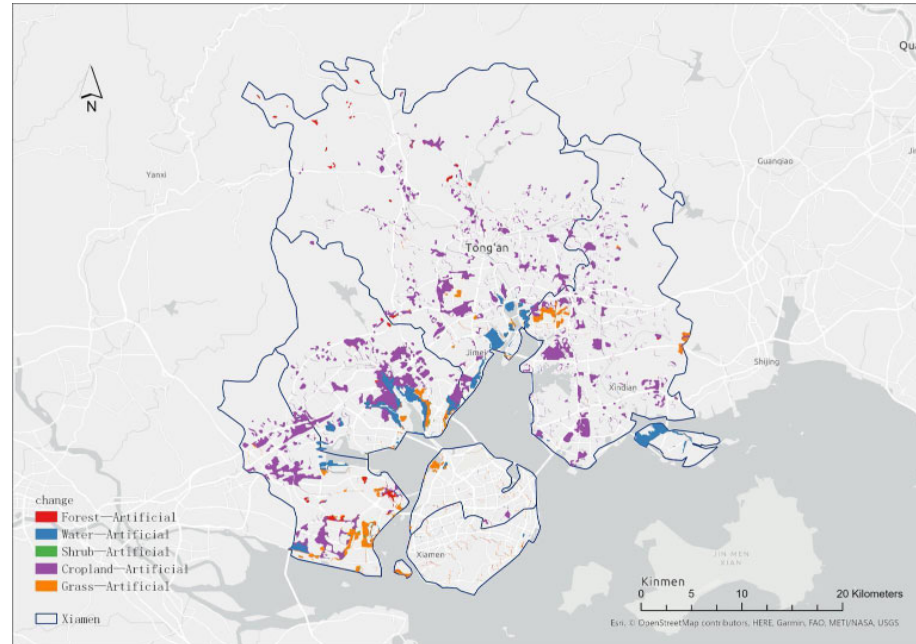


Figure 5.2.3 Conversion map of artificial surface from other land types

6. Eco-environmental quality assessment

6.1. RSEI Model

6.1.1. Principle of the RSEI Model

Remote Sensing Based Ecological Index (RSEI) is a method based entirely on remote sensing image element extraction (Xu and et al.,2019). Through the integration of four index elements (Greenness, Wetness, Heat, and Dryness), it can realize the evaluation of urban ecological status. The four index factors of the RSEI model are greenness (NDVI), humidity (WET), heat (LST), and dryness (NDSI). The functional expression of the RSEI model is:

$$RSEI = (Greenness, Wetness, LST, NDSI)$$

$$RSEI = f(NDVI, WET, LST, NDSI)$$

6.1.2 Indicator selection

(1) Greenness

The Normalized Difference Vegetation Index (NDVI) was used to monitor changes in vegetation growth and the ecological environment. The index can reflect the growth status of plants in urban areas, including vegetation growth rate, leaf area index, and vegetation coverage density.

$$NDVI = \frac{\rho_4 - \rho_3}{\rho_4 + \rho_3}$$

where ρ_4 is the reflectivity in the near-red band, and ρ_3 is the reflectivity in the red band.

(2) Humidity

The humidity index (WET) (Sarah E.Darrah and et al.,2019)was used to monitor the humidity of soil, water and vegetation in the environment. [17] For the Landsat 8OLI image, the formula is:

$$WET = 0.1511\rho_1 + 0.1973\rho_2 + 0.3283\rho_3 + 0.3407\rho_4 - 0.7117\rho_5 - 0.4559\rho_7$$

(3) Heat

The heat indicator is the Land Surface Temperature (LST). Commonly used surface temperature inversion methods are atmospheric correction method, single-window algorithm, single-channel method, etc. This study uses the model of the Landsat user manual and the latest revised parameters of Chander et al.(Juan C. Jiménez-Muñoz et al.,2014) The calculation formula is:

$$L10 = gain \times DN + bias$$

$$T = K2 / \ln(K1 / L10 + 1)$$

Where L10 is the radiation value of the pixel in the 10-band thermal infrared band of the OLI data in the sensor, DN is the gray value of the pixel, gain and bias are the gain and bias value of the thermal infrared band respectively, which can be found in the header file of the remote sensing image. obtained in. K1 and K2 are calibration parameters, which can be obtained from the user manual. For OLI data,

$$K1 = 774.89W \cdot m - 2 \cdot ster - 1 \cdot \mu m - 1, K2 = 1321.08K$$

The temperature T calculated by the formula must be corrected for the specific emissivity to form the surface temperature LST:

$$LST = T / [1 + (\lambda T / P) \ln \epsilon]$$

where λ is the center wavelength of OLI 10 band ($\lambda=10.900\mu m$), $\rho=0.01438m \cdot K$; ϵ is the surface-specific emissivity

(4) Dryness

The main factors causing the "drying" of the urban surface are construction land and bare soil. Therefore, NDSI was selected as the dryness index in this study. (Xu H Q,2008)The Dryness Index (NDSI) is a combination of the Bare Soil Index (SI) and the Building Index (IBI)], each of which accounts for half of the weight. Calculated as follows:

$$NDSI = \frac{IBI + SI}{2}$$

$$IBI = \frac{2\rho_5 / (\rho_5 + \rho_4) - [\rho_4 / (\rho_3 + \rho_4) + \rho_2 / (\rho_2 + \rho_5)]}{2\rho_5 / (\rho_5 + \rho_4) + [\rho_4 / (\rho_3 + \rho_4) + \rho_2 / (\rho_2 + \rho_5)]}$$

$$SI = \frac{(\rho_3 + \rho_5) - (\rho_4 + \rho_1)}{(\rho_3 + \rho_5) + (\rho_4 + \rho_1)}$$

In the above formula, ρ_i represents the reflectivity of the corresponding band, and NDSI is the dryness index.

6.1.3 PCA Analysis

Principal Component Analysis (PCA) is a data compression method that selects a few uncorrelated multi-dimensional indicators from multiple variables through orthogonal linear transformation(Athos Agapiou,2020). Its biggest advantage is that the contribution of each principal component can be confirmed according to each index, redundant data information can be effectively eliminated, and the result deviation caused by human intervention can be avoided.

6.1.4. RSEI Model Building

Since the dimensions of the four indicators calculated by the formula are not uniform, before doing the principal component change, these indicators must be normalized, and their dimensions are unified to [0, 1], and then the PCA is calculated. The normalization formula of each indicator is:

$$NI_i = (I_i - I_{min}) / (I_{max} - I_{min})$$

In the above formula, NI_i is the normalized pixel value, and I_i , I_{max} , and I_{min} are the original value, maximum value, and minimum value of the i th pixel, respectively.

After normalization, the four indicators can be used for principal component analysis.

In order to facilitate the measurement and comparison of indicators, $RSEI_0$ can also be normalized:

$$RSEI = (RSEI_0 - RSEI_{0_{min}}) / (RSEI_{0_{max}} - RSEI_{0_{min}})$$

The results show that the value of the remote sensing ecological index is in the interval [0, 1]. When the RSEI value is closer to 1, the ecological environment quality is better.

6.2. PCA Result

From the result of Principal component analysis(Table 6.2.1)

- (1) In 9 years, the eigenvalue contribution rate of PC1 is more than 85%, indicating that PC1 has concentrated most of the characteristics of the four indicators;
- (2) All the four indexes have certain effects and loads on PC1, and they are not unstable like other characteristic components (PC2-PC4).
- (3) In PC1, NDVI Index and Wet are positive, indicating that they have a positive impact on the ecosystem, while LST and NDSI index representing heat and dryness are negative, indicating that they have a negative impact on the ecosystem, which is consistent with the actual situation.

Table 6.2.1 Principal component analysis results

| | 2013 | | | | 2014 | | | | 2015 | | | |
|----------------------------|--------|--------|--------|--------|--------|--------|--------|--------|--------|--------|--------|--------|
| | PC1 | PC2 | PC3 | PC4 | PC1 | PC2 | PC3 | PC4 | PC1 | PC2 | PC3 | PC4 |
| NDVI | 0.956 | 0.293 | 0.025 | 0.012 | 0.879 | 0.459 | 0.082 | -0.102 | 0.092 | 0.013 | 0.011 | -0.003 |
| WET | 0.071 | -0.155 | -0.979 | 0.104 | 0.083 | -0.259 | 0.920 | 0.282 | 0.022 | -0.084 | 0.995 | 0.031 |
| NDSI | -0.021 | 0.018 | 0.102 | 0.994 | -0.399 | 0.558 | 0.383 | -0.619 | -0.041 | 0.002 | 0.031 | -0.995 |
| LST | -0.284 | 0.943 | -0.172 | -0.005 | -0.248 | 0.641 | -0.020 | 0.726 | -0.127 | 0.988 | -0.859 | 0.004 |
| Eigenvalue | 0.087 | 0.007 | 0.007 | 0.003 | 0.095 | 0.011 | 0.002 | 0.004 | 0.086 | 0.004 | 0.004 | 0.001 |
| Percent eigenvalue% | 91.69 | 7.53 | 0.78 | 0.02 | 85.86 | 0.29 | 0.22 | 3.63 | 95.34 | 4.16 | 0.49 | 0.01 |

| | 2016 | | | | 2017 | | | | 2018 | | | |
|----------------------------|--------|--------|--------|--------|--------|--------|--------|--------|--------|--------|--------|--------|
| | PC1 | PC2 | PC3 | PC4 | PC1 | PC2 | PC3 | PC4 | PC1 | PC2 | PC3 | PC4 |
| NDVI | 0.976 | 0.217 | 0.021 | -0.004 | 0.991 | 0.128 | 0.014 | 0.001 | 0.985 | 0.170 | 0.011 | 0.006 |
| WET | 0.069 | -0.218 | -0.973 | -0.033 | 0.043 | -0.426 | 0.904 | 0.009 | 0.037 | -0.150 | -0.986 | 0.057 |
| NDBSI | -0.007 | 0.008 | 0.032 | -0.999 | -0.002 | 0.004 | -0.008 | 0.999 | -0.008 | 0.008 | 0.056 | 0.998 |
| LST | -0.207 | 0.951 | -0.228 | 0.002 | -0.122 | 0.896 | 0.428 | -0.005 | -0.008 | 0.008 | 0.056 | 0.998 |
| Eigenvalue | 0.078 | 0.004 | 0.006 | 0.002 | 0.079 | 0.003 | 0.001 | 0.003 | -0.167 | 0.973 | -0.154 | -0.007 |
| Percent eigenvalue% | 93.68 | 5.59 | 0.74 | 0.03 | 95.18 | 3.55 | 1.27 | 0.04 | 95.53 | 3.98 | 0.48 | 0.01 |

| | 2019 | | | | 2020 | | | | 2021 | | | |
|----------------------------|--------|--------|--------|--------|--------|--------|--------|--------|--------|--------|--------|--------|
| | PC1 | PC2 | PC3 | PC4 | PC1 | PC2 | PC3 | PC4 | PC1 | PC2 | PC3 | PC4 |
| NDVI | 0.993 | 0.109 | -0.033 | -0.001 | 0.983 | 0.182 | -0.035 | 0.004 | 0.993 | 0.120 | -0.021 | 0.009 |
| WET | 0.056 | -0.456 | -0.191 | 0.868 | 0.077 | -0.228 | -0.970 | -0.024 | 0.049 | -0.239 | 0.967 | 0.067 |
| NDBSI | -0.005 | 0.096 | -0.981 | -0.162 | -0.006 | 0.006 | 0.002 | -0.999 | -0.012 | 0.017 | -0.064 | 0.998 |
| LST | -0.090 | 0.878 | 0.011 | 0.469 | -0.168 | 0.956 | -0.239 | 0.001 | -0.111 | 0.963 | 0.244 | -0.002 |
| Eigenvalue | 0.078 | 0.004 | 0.001 | 0.001 | 0.077 | 0.006 | 0.001 | 0.001 | 0.080 | 0.003 | 0.001 | 0.001 |
| Percent eigenvalue% | 93.96 | 4.32 | 0.21 | 1.71 | 92.15 | 6.87 | 0.98 | 0.01 | 96.04 | 3.09 | 0.87 | 0.01 |

6.3. Evaluation of Ecological Environment

This study divides the study area into five ecological levels based on the RSEI score, according to the Environmental Protection Industry Standards of the People's Republic of China(Trial Implementation) (2006). The standards are as follows: Level 1(0 < RSEI ≤0.2), Level 2 (0.2 < RSEI ≤0.4), Level 3 (0.4 < RSEI ≤0.6), Level 4(0.6 < RSEI ≤0.8) and Level 5(0.8 < RSEI ≤1), with Level 1 indicating the worst ecological environment, while Level 5 indicating the best ecological environment. The result of level classification from 2013 to 2021 is displayed in Table 6.3.1.

As the result shows, in 2013, Xiamen had the best ecological quality, with an area of 767.54 square kilometers (48.61%) in the 'Level 5' (excellent) and 'Level 4'(good) grades, while only 12.65% of the area

had poor (Level 1) ecological quality. After nearly 10 years of development, however, in 2021, the proportion of 'Level 1' (poor) areas has increased by 112% 2021, while the proportion of areas with Level 5(excellent) and Level 4(good) grades has decreased by 10%. In general, the land area of 'Level 1' and 'Level 2' increased in a fluctuating manner, while the land area of 'Level 4' and 'Level 5' decreased, indicating that the ecological quality of Xiamen has declined gradually in the last decade as urbanization progressed.

Table 6.3.1 Grading table of ecological environment evaluation

| Level | 2013 | | 2014 | | 2015 | |
|---------|-------------------------|----------------|-------------------------|----------------|-------------------------|----------------|
| | Area (km ²) | Proportion (%) | Area (km ²) | Proportion (%) | Area (km ²) | Proportion (%) |
| Level 1 | 199.75 | 12.65 | 188.05 | 11.91 | 300.91 | 19.06 |
| Level 2 | 347.71 | 22.02 | 426.95 | 27.04 | 253.23 | 16.04 |
| Level 3 | 264.13 | 16.72 | 289.42 | 18.33 | 251.10 | 15.90 |
| Level 4 | 326.17 | 20.66 | 395.05 | 25.02 | 384.61 | 24.36 |
| Level 5 | 441.37 | 27.95 | 279.66 | 17.71 | 389.27 | 24.65 |

| Level | 2016 | | 2017 | | 2018 | |
|---------|-------------------------|----------------|-------------------------|----------------|-------------------------|----------------|
| | Area (km ²) | Proportion (%) | Area (km ²) | Proportion (%) | Area (km ²) | Proportion (%) |
| Level 1 | 229.89 | 14.50 | 183.11 | 11.59 | 305.88 | 19.37 |
| Level 2 | 328.80 | 20.82 | 498.89 | 31.59 | 296.09 | 18.75 |
| Level 3 | 300.42 | 19.03 | 259.39 | 16.43 | 254.13 | 16.09 |
| Level 4 | 496.00 | 31.41 | 288.17 | 18.25 | 301.49 | 19.09 |
| Level 5 | 224.02 | 14.19 | 349.31 | 22.12 | 421.54 | 26.69 |

| Level | 2019 | | 2020 | | 2021 | |
|---------|-------------------------|----------------|-------------------------|----------------|-------------------------|----------------|
| | Area (km ²) | Proportion (%) | Area (km ²) | Proportion (%) | Area (km ²) | Proportion (%) |
| Level 1 | 345.89 | 21.91 | 300.42 | 19.03 | 423.02 | 26.79 |
| Level 2 | 302.16 | 19.14 | 374.21 | 23.70 | 274.62 | 17.39 |
| Level 3 | 251.09 | 15.90 | 292.33 | 18.51 | 268.19 | 16.98 |
| Level 4 | 326.75 | 20.69 | 441.45 | 27.96 | 301.33 | 19.08 |
| Level 5 | 353.25 | 22.37 | 170.73 | 10.81 | 311.98 | 19.76 |

RSEI grading map in Figure 6.3.2 shows that the ecological quality of 'Level 1' and 'Level 2' regions is mostly distributed in urban built-up areas. The areas with poor ecological environments are concentrated in the north of Xiamen Island and the coastline area. From the perspective of time series, the urban

expansion of Xiamen presents an expansion trend from the coastal plain in the southeast to the hills and low mountains in the northwest.

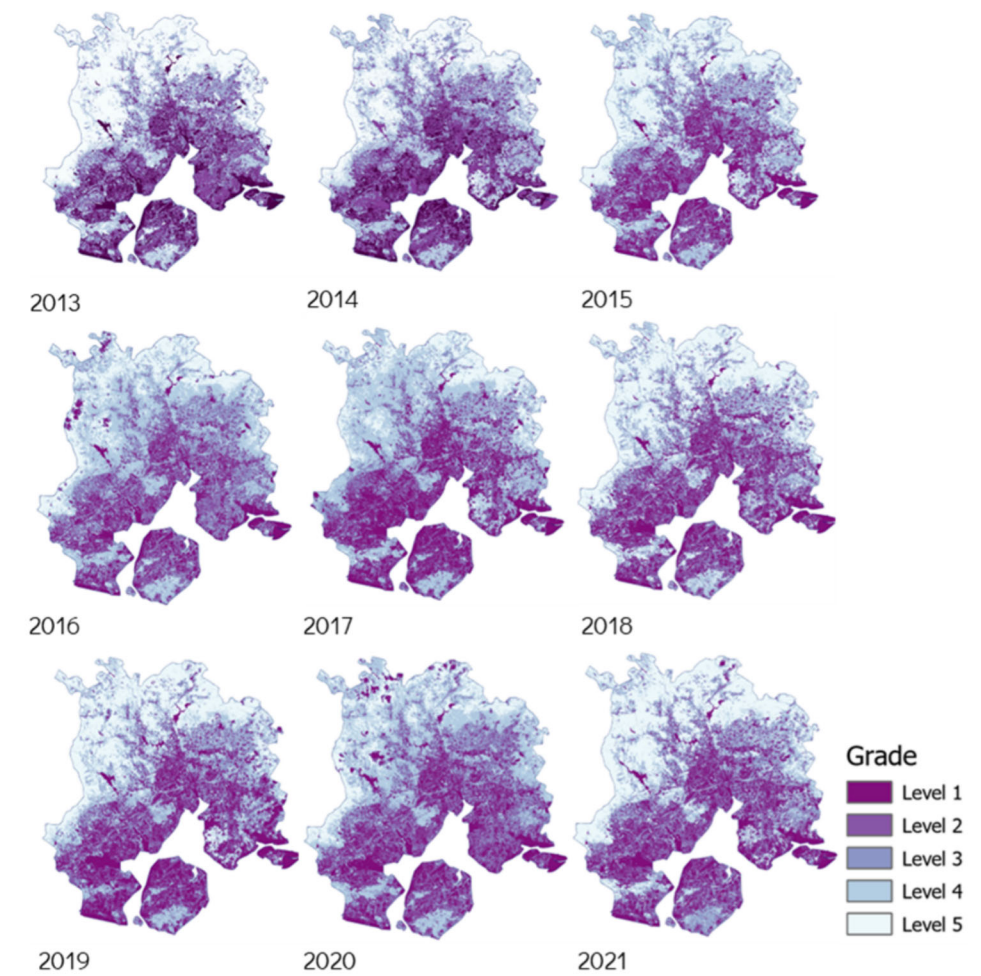


Figure 6.3.2 Grade evaluation map

To better understand the transformation of the ecological environmental quality in Xiamen between 2013 and 2021, the difference between the RSEI level in 2021 and 2013 was made and mapped in Figure 6.3.3. When the level difference is 0, it means that the region's environmental quality has not changed greatly. When the level difference is negative, it means that the ecological environment quality of the region has become worse than before, and when the level difference is positive, it means that the ecological environment of the region has improved. The greater the level difference, the larger the scale of environmental quality transformation is.

As shown in Table 6.3.4, the area of ecological environment quality in Xiamen got better was 240.79 square kilometers. The area of ecological environment quality got worse at 440.35 square kilometers, almost twice the improvement area. The area of ecological environment quality that did not change was

897.99 square kilometers. Such a result reveals that the ecological environment quality of Xiamen city has obviously declined in the past ten years. The ecological quality in Xiamen Island, where the urban center is located, decreased slightly. The most excessive-quality deterioration occurs in the urban expansion boundary, while the improvement area concentrates in the southwest part of Xiang'an District.

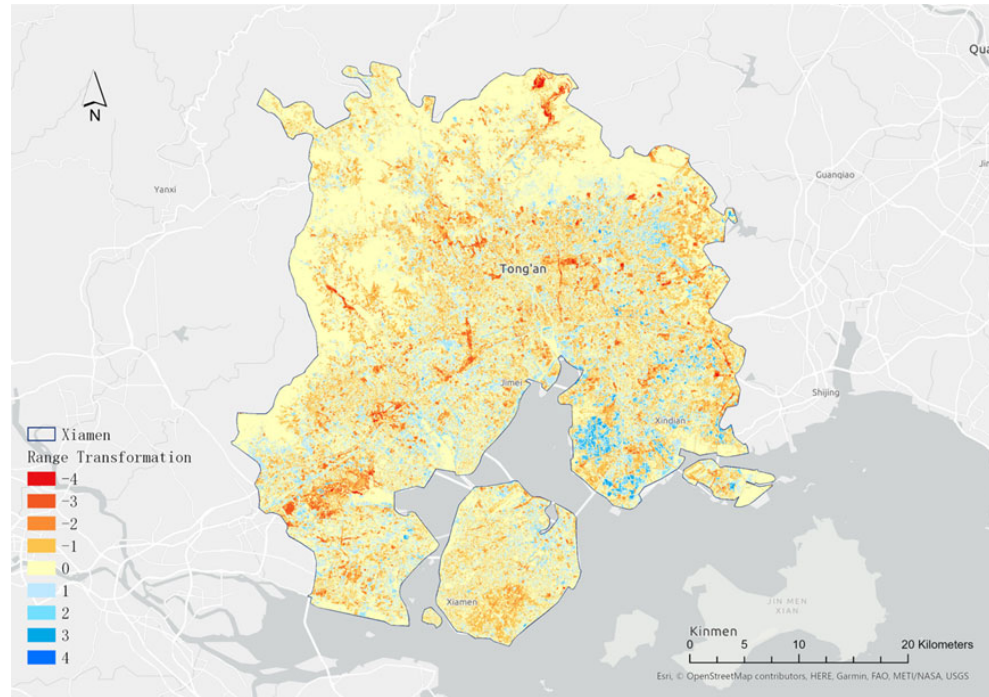


Figure 6.3.3 Transformation of ecological environmental quality level

Table 6.3.4 Measurement table of ecological environment grade change in Xiamen from 2013 to 2021

| Category | Level Difference | Level Area (km ²) | Category Area (km ²) |
|---------------|------------------|-------------------------------|----------------------------------|
| Better | 4 | 0.34 | 240.79 |
| | 3 | 9.39 | |
| | 2 | 32.42 | |
| | 1 | 198.64 | |
| Same | 0 | 897.99 | 897.99 |
| Worse | -1 | 345.58 | 440.35 |
| | -2 | 73.01 | |
| | -3 | 19.33 | |
| | -4 | 2.43 | |

6.4. Case study of ecological change

With continuous urbanization, human activities are constantly changing the urban ecological environment. This study selected examples in Xiamen as a case study to explore the impact of transportation development, industrial development, and environmental protection strategy on the urban ecological environment. Landsat8 OLI remote sensing image in 2013 and the Tencent Map satellite image in 2021

are selected to compare and analyze the transformation of the same region in the study period, and the remote sensing ecological level transformation map is applied to verify the ecological changes in the region.

In Figure 6.4.1, the red circled area of the transformation map is the 22,800 mu of high-standard farmland built by the Xiamen Municipal Government in 2018. The green flat area of the larger plot (urban farmland land) was bare land or construction land nine years ago, but after government planning in recent years, the bare land has gradually been replaced by urban nurseries and cropland. Through photosynthesis and transpiration, vegetation can effectively absorb harmful gasses in the air, such as sulfides and car exhausts; it also has a bactericidal effect, absorbing dust and reducing bacterial carriers, thus promoting a virtuous cycle of urban ecology and contributing to the construction of a green ecology in the city. The case of high-standard farmland shows that the government's environmental protection strategy can help improve ecological quality.



Figure 6.4.1 Before and after comparison of high-standard farm remote sensing images

In Figure 6.4.2, the area circled in red on the transformation map is the logistics distribution center of Xiamen, which is home to several large courier distribution points such as Baishi, Shentong, and Zhongtong. With the development of the express industry and road development, it can be found from the remote sensing images that in 2013, this area was covered by a large amount of grass, shrub, and forest. But in 2021, the vegetation coverage is basically zero. During the development process, ecological land was converted into bare land and hypothetical land, and the formation of a large amount of impervious surface made the land regulation ability and air quality of this area deteriorate, damaging the ecological environment. The ecological environment is extremely poor, with a transformation value of -4, indicating that industrial development can damage the ecological environment.

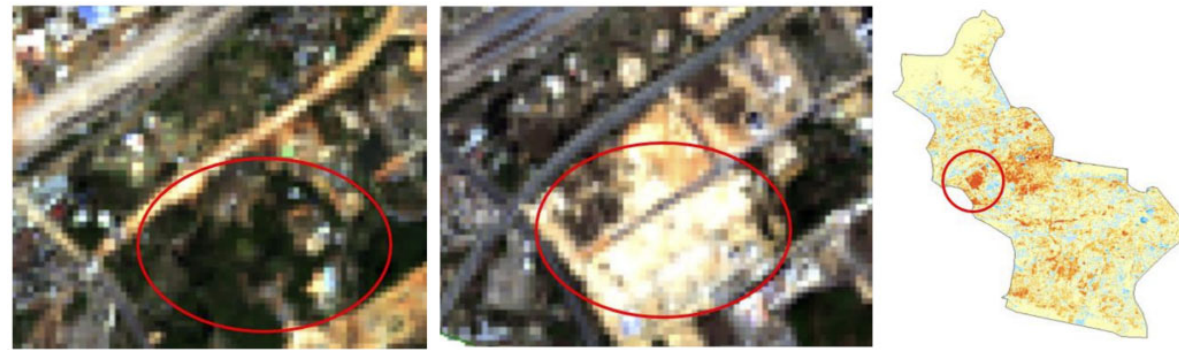


Figure 6.4.2 Before and after comparison of remote sensing images of logistics distribution centers

In Figure 6.4.3, the area in the red circle is Xiamen Railway Station. Due to the redevelopment of the main station building and the expansion of the south station building in the last decade, together with the rise of the surrounding commercial area, the area of construction land gradually increased, with impervious surfaces replacing the previously cultivated land and a small portion of woodland. Moreover, the commissioning of the new station platform has increased the traffic flow on the original station, together resulting in a significant decline in the ecological quality of the surrounding environment.



Figure 6.4.3 Before and after comparison of remote sensing images of Xiamen Station

In Figure 6.4.4, the study area is Xiamen North Station. Due to the expansion of the infrastructure of the station, some of the nearby grassland and arable land have been occupied for construction, resulting in an increase in the impervious surface area. The development of the railway industry and the increase in the number of railway lines has led to a change in the nature of the land surface, which has also led to a level difference of around -4, making this area the area with the most obvious deterioration in ecological quality in Jimei District. From the Xiamen Station and Xiamen North Station case, it can be concluded that transport development might increase impervious surfaces and bring a negative impact on ecology.



Figure 6.4.4 Before and after comparison of remote sensing images of Xiamen North Station

7. Conclusion

This study takes Xiamen as the study area and selects GlobeLand 30 land use data for the two periods of 2010 and 2020 and Landsat8 OLI data for nine years to study the urban expansion characteristics and evaluate the spatial and temporal changes in the ecological environment of Xiamen in the last decade. The following conclusions can be reached after the remote sensing image processing, level classification, and evaluation.

First, over the nine years from 2013 to 2021, Xiamen's urban expansion follows a pattern of gradual expansion from coastline plains in the southeast to the hilly terrain in the northwest. Second, the expansion of the construction area in Xiamen was achieved mainly through the occupation of cropland and ecological land. Due to the need for agricultural development, when the original cropland is converted to construction land, new ecological land will be reclaimed for cultivation to maintain agricultural production. Third, from 2013 to 2021, the average level of RSEI decreased from 3.29 to 2.87. With the development of urbanization, the quality of the ecological environment in Xiamen is gradually declining.

In summary, urbanization has a significant impact on the quality of the urban ecological environment. When ecological land is converted to impermeable surfaces, the original urban ecology is altered, and the environment becomes less regulated, resulting in air pollution, urban flooding and drought, and the heat island effect. This study shows that ecological land, such as woodland and grassland, positively affects urban ecology, as vegetation can hold soil in place, absorb airborne dust, purify noise, and produce oxygen. Nowadays, with the development of cities, government departments should pay attention to the harmonious development of the urban environment and urban economy to promote economic development and urbanization while minimizing the damage to the ecological environment.

Besides, we are also aware that this study has limitations. As the results of the RSEI calculation are strongly influenced by time and climate, images of the same month with lower cloudiness should be selected for further study.

Reference

- Agapiou, A. (2020) 'Evaluation of Landsat 8 OLI/TIRS Level-2 and Sentinel 2 Level-1C Fusion Techniques Intended for Image Segmentation of Archaeological Landscapes and Proxies', *Remote Sensing*, 12(3), p. 579. doi:10.3390/rs12030579.
- Brueckner, J.K. (2000) 'Urban expansion: Diagnosis and Remedies', *International Regional Science Review*, 23(2), pp. 160–171. doi:[10.1177/016001700761012710](https://doi.org/10.1177/016001700761012710).
- Darrah, S.E. et al. (2019) 'Improvements to the Wetland Extent Trends (WET) index as a tool for monitoring natural and human-made wetlands', *Ecological Indicators*, 99, pp. 294–298. doi:10.1016/j.ecolind.2018.12.032.
- Hu, X. and Xu, H. (2018) 'A new remote sensing index for assessing the spatial heterogeneity in urban ecological quality: A case from Fuzhou City, China', *Ecological Indicators*, 89, pp. 11–21. doi:[10.1016/j.ecolind.2018.02.006](https://doi.org/10.1016/j.ecolind.2018.02.006).
- Irwin, E.G. and Bockstael, N.E. (2007) 'The evolution of urban expansion: Evidence of spatial heterogeneity and increasing land fragmentation', *Proceedings of the National Academy of Sciences*, 104(52), pp. 20672–20677. doi:[10.1073/pnas.0705527105](https://doi.org/10.1073/pnas.0705527105).
- Jimenez-Munoz, J.C. et al. (2014) 'Land Surface Temperature Retrieval Methods From Landsat-8 Thermal Infrared Sensor Data', *IEEE Geoscience and Remote Sensing Letters*, 11(10), pp. 1840–1843. doi:10.1109/LGRS.2014.2312032.
- Pettorelli, N. et al. (2005) 'Using the satellite-derived NDVI to assess ecological responses to environmental change', *Trends in Ecology & Evolution*, 20(9), pp. 503–510. doi:[10.1016/j.tree.2005.05.011](https://doi.org/10.1016/j.tree.2005.05.011).
- State Environmental Protection Administration.(2006). Environmental Protection Industry Standards of the People's Republic of China (Trial Implementation) : HJ/T192–2006. Beijing : China Environmental Science Press
- Tang, J., Wang, L. and Yao, Z. (2006) 'Analyzing Urban expansion Spatial Fragmentation Using Multi-temporal Satellite Images', *GIScience & Remote Sensing*, 43(3), pp. 218–232. doi:[10.2747/1548-1603.43.3.218](https://doi.org/10.2747/1548-1603.43.3.218).
- Xu, Y. et al. (2018) 'Building Extraction in Very High Resolution Remote Sensing Imagery Using Deep Learning and Guided Filters', *Remote Sensing*, 10(1), p. 144. doi:[10.3390/rs10010144](https://doi.org/10.3390/rs10010144).
- Xu, H. (2008) 'A new index for delineating built-up land features in satellite imagery', *International Journal of Remote Sensing*, 29(14), pp. 4269–4276. doi:10.1080/01431160802039957.
- Xu, H. et al. (2019) 'Detecting Ecological Changes with a Remote Sensing Based Ecological Index (RSEI) Produced Time Series and Change Vector Analysis', *Remote Sensing*, 11(20), p. 2345. doi:10.3390/rs11202345.